

Surface Chemistry of CH₃Br and Methyl Modified by Copper Deposition on Ru(001)

T. Livneh[†] and M. Asscher*

Department of Physical Chemistry and the Farkas Center for Light Induced Processes, The Hebrew University, Jerusalem 91904, Israel

Received: December 3, 1998; In Final Form: March 18, 1999

The chemistry of methyl bromide on Cu/Ru(001) has been studied utilizing work function change ($\Delta\phi$) and temperature-programmed desorption (TPD) measurements. The remarkable modification in the methyl fragments dehydrogenation at the completion of a single copper layer and the significant difference in reactivity of the Cu(2 ML)/Ru(001) or Cu(111) surfaces are the focus of this study. A decrease in work function at the completion of 1 ML CH₃Br of 2.15 ± 0.02 eV and 1.33 ± 0.05 eV was measured, respectively, for Ru(001) and Cu(2 ML)/Ru(001) held at 82 K. Methyl bromide does not dissociate upon adsorption on clean or the copper-covered surfaces, and it is bound with the bromine down. Copper modifies the reactivity of the Ru substrate, gradually decreasing the dissociated fraction of CH₃Br from 0.55 of the initial one monolayer on clean Ru(001) to 0.06 on Cu(2 ML)/Ru(001), probably because of defects in the copper layer. The methyl fragment dehydrogenation rate slows as the copper coverage increases. At a narrow copper coverage range between 0.8 and 0.95 ML, adsorbed hydrogen and methyl fragments coexist on the surface in the temperature range 230–280 K. Sequential decomposition channels of the parent molecules and the methyl fragment lead to a unique enhancement of methane production rate, this on the account of further hydrocarbon dehydrogenation, as reflected in both Δp and $\Delta\phi$ TPD measurements. Methane is formed on top of copper terraces as a result of “spill-over” of both methyl and hydrogen atoms, similar to the chemistry over Cu(111) and Cu(110) single-crystal surfaces. The dipole moment of adsorbed methyl is reported here for the first time on metal surfaces, being 0.48 D on top of Cu(2 ML)/Ru(001).

I. Introduction

Interest in bimetallic catalysts had been motivated by the commercial success of these systems. This success results from the improved ability to control the catalytic activity and selectivity by tailoring the catalyst's composition. One of the most extensively investigated bimetallic systems is Cu/Ru.^{1–4} Cu/Ru catalysts have been used to control catalytic activity and selectivity in the Fischer–Tropsch reaction.^{1,3,5,6} The addition of Cu to Ru induces formation of longer chains of alkane.³

A key issue in these studies is the relative role of “ligand” (electronic) vs “ensemble” (morphological) effects in identifying the catalytic behavior. Ensemble effect is often associated with a simple blocking of sites adjacent to the active one. By reduction of the number of vacant sites, the surface is deactivated. Reactions that require a large ensemble of active sites can be selectively suppressed, leaving only small ensemble reactions. In the case of Cu/Ru(001) at 300 K copper forms islands^{7–9} and blocks the chemisorption of both H₂¹⁰ and CO^{11,12} on the Ru(001) surface.

Formation of the bond between the two different metals leads to electron polarization toward the element with the larger fraction of empty states in its valence band and is accompanied by a large perturbation in the electronic properties of the metals. The resulting electronic modification can dramatically alter surface chemical (catalytic) properties of the bimetallic system.^{1,13–19} Strong electronic perturbation between the metal overlayer and the underlying transition metal were observed in

X-ray photoelectron spectroscopy (XPS) studies of Cu/Ru(001)¹⁶ as in other bimetallic systems.^{15a}

By use of scanning tunneling spectroscopy (STM), the modified electronic structure was found to induce perturbations, which extend up to 50–100 Å away. They are observed at the step edges or adatoms that may alter adsorbate binding energy and generate new adsorption sites.^{20,21} Step edges of copper islands on Ru (001) were found to trap H and CO and thus reduce the diffusion coefficient of hydrogen on Ru(001) by 3 orders of magnitude by depositing only 0.2 ML copper.²² These new adsorption sites are characterized by a substantially different local work function, probed by photoemission of adsorbed xenon (PAX).^{17–19}

Cu is immiscible in Ru, which circumvents the complication of determining the three-dimensional composition. It is known also to grow epitaxially on the clean Ru(001), forming a pseudomorphic film in the first layer.^{7–9} The pseudomorphic growth implies that the Cu–Cu bond distances are strained 5.5% beyond the equilibrium distances found for bulk copper. The second layer is contracted practically to the interatomic distance of Cu(111) in one direction, while in the perpendicular direction the Cu atoms are still in registry with the Ru(001) atoms. The growth mechanism up to 4 ML of Cu is “layer by layer”. The well-characterized surface of the Cu/Ru(001) system^{7–9,23–25} makes it an ideal model bimetallic catalyst.

Although adsorption and desorption kinetics of several adsorbates have been studied on the Cu/Ru(001) system,^{10–12} very few investigations have examined the dependence of the adsorption and dissociation mechanism on the copper coverage. Considerable insight into the catalytic processes can be gained by these investigations, although some discrepancy is found

[†] Current address: Department of Physical Chemistry, Nuclear Research Center, Negev, P.O. Box 9001, Beer Sheva, Israel.

between the "real" polycrystalline Cu/Ru catalyst powder and the smooth Ru(001) deposited by copper atoms.¹⁷ For example, in the C₂H₄/Cu/Ru(001) system²⁶ the copper deposition generated new adsorption sites that have mixed Cu and Ru character. The influence of these new sites on the dehydrogenation pathways of ethylene is a key issue for understanding the carbide layer formation, which is the final stage of the dehydrogenation sequence.

Recently, there had been considerable interest in the adsorption of methyl halides on single-crystal surfaces.²⁷ The importance of these molecules as a model for surface alkylation and in particular their damaging role in atmospheric reactions motivated these studies. Under ultrahigh vacuum (UHV) conditions the reactivity toward C–X bond cleavage follows the trend I > Br > Cl on several catalytic metal surfaces. Studies of Ru(001) indicate that CH₃I dissociates completely upon adsorption at 100 K.²⁸ CH₃Br starts to only partially (55%) dissociate at 125 K,²⁹ and CH₃Cl does not dissociate at all.³⁰ On Cu(111) CH₃I starts to partially dissociate at 140 K,³¹ but CH₃Br does not.^{32,33}

From the three methyl halides the most interesting one in terms of its catalytic properties is CH₃Br because of its rather different reactivity on copper and ruthenium. In the present study the interaction of the methyl bromide with the bare Ru(001) surface is compared to the Cu(0–2ML)/Ru(001) surface in terms of characteristic adsorption sites and reactivity. The chemistry of the methyl fragment is thus used as a probe of the gradually changing nature of the metallic surface as the copper coverage increases. This reactive probe provides a complementary and a rather different viewpoint of the surface compared to the standard use of CO as a sensor.^{15a}

II. Experimental Section

The experiments described here were performed in a UHV chamber with a base pressure of 3×10^{-10} Torr obtained by a turbomolecular pump (240 L/s). A sputter gun (Ar⁺ ions at 600 V and sample current of 8 μ A) to clean the Ru(001) surface and a quadrupole mass spectrometer (QMS VG MASSTORR DX) for Δp TPD spectra were used. The QMS was surrounded by a Pyrex shroud with a 5 mm diameter aperture to minimize detection of desorbing molecules from surfaces other than the sample. A kelvin probe (Besocke type S) was employed to monitor the work function change ($\Delta\phi$). Both TPD and work function changes were measured as a function of crystal temperature using the same routine. A computer-controlled ac resistive heating method could, at the same time, control the heating rate or stabilization temperature (± 0.5 K) and collect data via an A/D converter either from the quadrupole to obtain Δp -TPD or from the kelvin probe controller to obtain $\Delta\phi$ TPD spectra.

The Ru(001) sample (a square piece, 8 mm \times 8 mm, 1.5 mm thick) was cut from a single-crystal rod to within $\pm 1^\circ$ of the (001) crystallographic orientation and then polished by diamond paste having particles of 0.25 μ m. Sample cleaning in UHV was described elsewhere.²⁹ LEED from the clean and annealed surface showed a very sharp hexagonal pattern. The sample was attached to a liquid nitrogen reservoir via copper feedthroughs directly welded to the bottom of the Dewar. The ac resistive heating of two 0.5 mm diameter tantalum wires, between which the sample is spot-welded, was employed to control the sample temperature. (W5% Re)–(W26% Re) thermocouple wires spot-welded to the edge of the ruthenium sample were used for sample temperature determination and control.



Figure 1. STM image of 0.3 ML of Cu deposited on Ru(001) at 650 K, recorded by Ammer and co-workers.^{9a} Image conditions are 190 nm \times 200 nm, 1 nA, and -60 mV bias voltage. The darker areas are of the Ru(001) substrate, and the bright stripes are of the copper terraces.

CH₃Br (99.5% pure) was further purified by a few freeze–pump–thaw cycles to eliminate any noncondensable residual gases. Exposure was done by filling the chamber through a leak valve to the desired pressure, with the uncorrected ion gauge signal transmitted to a computer and converted to Langmuir units (1 L = 10^{-6} Torr s).

Copper was evaporated onto the Ru(001) sample from a resistively heated Ta wire wrapped in high-purity Cu wire (99.999%). The Ta filament was covered by a Pyrex shroud with a 5 mm diameter aperture. The Cu source was thoroughly degassed prior to deposition and was controlled by monitoring the voltage drop across the Ta wire at constant current. The copper coverage was determined by TPD after each experiment. The pressure rise during copper evaporation was routinely $(1-2) \times 10^{-10}$ Torr. The sample was held during evaporation at 640 K in order to avoid CO adsorption and to produce a well-annealed surface, thus avoiding three-dimensional clustering of copper on the Ru(001) surface.^{7,9}

III. Results and Discussions

1. Cu/Ru(001). Deposition of copper on Ru(001) has been extensively studied by STM^{7–9} and by other methods.^{23–25} Up to a coverage of at least four monolayers (ML), the observed growth behavior is compatible with both layer-by-layer and layer/3D-cluster growth modes, strongly dependent on crystal temperature and deposited atom flux. At a surface temperature of 300 K, second-layer islands are formed already around $\theta_{\text{Cu}} = 0.8$ ML, and at coverages higher than 1.2 ML third-layer islands are also observed. Annealing to 520 K was found to dissolve the third layer into the first two layers. In conclusion, when adsorption temperature is above 500 K, the growth mode at submonolayer levels is always by a step flow mechanism.^{7–9}

In Figure 1 an STM image is presented of 0.3 ML Cu/Ru(001) deposited at 650 K, as taken by Ammer et al.^{9a} The deposited copper atoms (bright stripes) are mobile enough to be captured by the Ru(001) step edges. Further Cu deposition results in a step flowlike growth mode, which is supposed to wet the

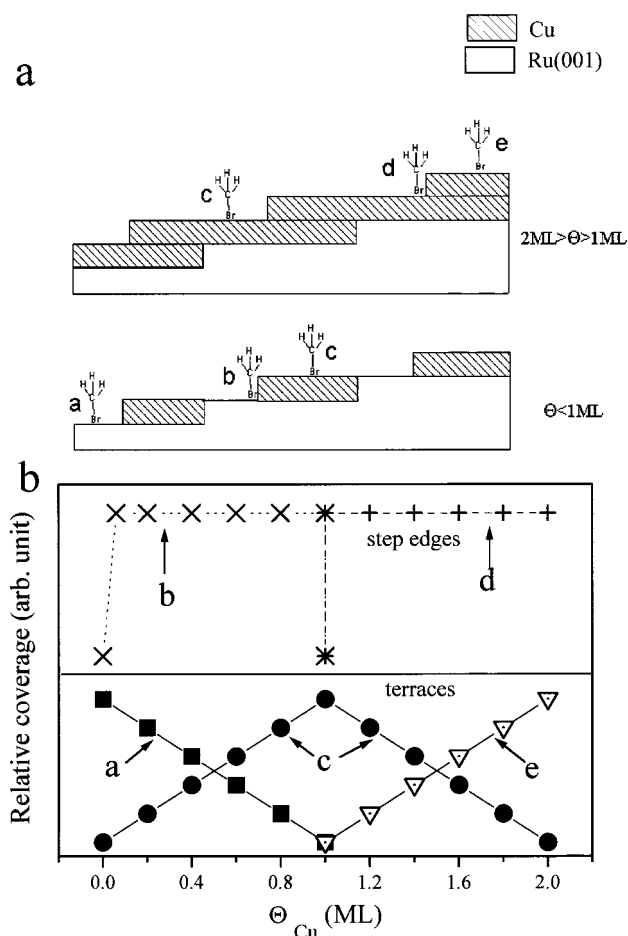


Figure 2. (a) Scheme of the Cu/Ru(001) surface representing the typical sites for a CH₃Br molecule when adsorbed on Cu(0–2 ML)/Ru(001). The copper was deposited at a crystal temperature of 640 K. The copper coverage regimes are indicated as follows: (a) Ru(001) surface, (b) Cu(1 ML)/Ru(001) step edges, (c) Cu(1 ML)/Ru(001) terraces, (d) Cu(2 ML)/Ru(001) step edges, (e) Cu(2 ML)/Ru(001) terraces. (b) Distribution of a–e sites as a function of copper coverage.

substrate surface completely at 1 ML of Cu. The step flow regime is preserved up to 3–4 ML of Cu even if individual Cu islands do exist on the surface. However, despite the layer-by-layer growth, small bare Ru patches were still observed under experimental conditions similar to those of the present work, up to at least 1.4 ML, believed to be generated around defect sites.²⁶ Furthermore, even high annealing temperatures could not completely eliminate these rather stable vacancies within the first copper layer on the Ru(001) surface.^{8b}

On the basis of the growth scheme depicted from the STM study described above in Figure 1, we have marked specific adsorption sites of the CH₃Br molecules on the gradually copper-covered Ru(001) surface. The various sites are classified into five groups, sketched in Figure 2a, as a function of copper coverage: (a) clean Ru(001) terraces, (b) Cu(1 ML)/Ru(001) step edges, (c) Cu(1 ML)/Ru(001) terraces, (d) Cu(2 ML)/Ru(001) step edges, and (e) Cu(2 ML)/Ru(001) terraces. The differences in the morphology of the surface observed as the copper coverage increases above 2 ML^{7–9} are not reflected in the parent molecule's Δp TPD spectra, which remains unchanged. Therefore, the e sites are taken to represent the Cu(>2 ML)/Ru(001) as well. The density of the various types of sites as a function of copper coverage is shown in Figure 2b. The model described in this figure is valid under the assumption that the step edge concentration is constant. However, we note

that the terraces are not necessarily equally spaced, which might result in sites of type d at copper coverages less than 1 ML.

Temperature-programmed desorption spectra of copper from Ru(001) are well documented in the literature^{23,25a} and clearly separate the first from the second layers. We have used the integrated TPD of copper in order to determine the copper coverages at an accuracy of 5%. The work function change of the Ru(001) surface as a function of copper coverage, calibrated against the integrated area under the corresponding Δp TPD peak, has been measured (not shown). This is in order to evaluate the work function contribution by the methyl bromide on the copper-covered surface. The work function decreases monotonically down to -0.72 eV at 1 ML of copper, and then it is kept fixed up to 2 ML and above. These numbers agree very well with the continuous work function change measurements taken during copper deposition on the same surface and reported previously.^{25a}

This observation demonstrates that the work function of a metallic overlayer does not necessarily correlate with the chemical reactivity on this layer. As will be demonstrated below, the unique chemistry of methyl fragments on Cu(1 ML)/Ru(001), which is rather different from the chemistry on Cu(111), has been recorded.

2. CH₃Br on Cu(2 ML)/Ru(001). Characterization of the adsorption state of methyl bromide was obtained by a combination of work function change measurements during adsorption at 82 K followed by Δp TPD at the molecular mass of CH₃Br ($m/e = 94$). These studies indicate that the molecule does not dissociate upon adsorption at this temperature on the clean Ru(001).²⁹ We have used these techniques to study and compare the effect of 2 ML of copper on the same surface in terms of the molecular behavior.

Work function change measurements during adsorption of methyl bromide on the Cu(2 ML)/Ru(001) surface reveal behavior very similar to that previously reported on the clean Ru(001)²⁹ and are shown in Figure 3. The first monolayer induces a decrease of $1.33 \text{ eV} \pm 0.05$ (compared with $2.15 \text{ eV} \pm 0.02$ on the clean Ru(001)), while the second layer causes a smaller increase, again similar but at a smaller magnitude compared with the clean ruthenium. This behavior has been interpreted in terms of a molecular adsorption geometry where the first-layer molecules adsorb with the bromine facing the metal surface while in the second layer it is predominantly adsorbed in the opposite geometry.²⁹ The overall smaller magnitude of the work function change that was found on the copper-covered surface suggests that the adsorption geometry on this surface is characterized by a higher level of disorder. Probably a significant fraction of the molecules are tilted with respect to the surface normal, in agreement with reports on the geometry of this molecule on Cu(111)³² and Cu(10 ML)/Ru(001).³⁹

It is interesting to note that the alternating adsorption geometry within the first layers of methyl bromide on the clean Ru(001), inferred from the work function change data, is consistent with the molecular crystal structure.³⁴ The behavior on the copper-covered surface suggests that the interaction of methyl bromide with copper induces geometrical changes within the first layer, which prevent the growth of well-ordered bulklike crystal.

Once the methyl bromide molecules adsorb on the 2 ML copper-covered ruthenium surface, Δp TPD measurements at the molecular mass were performed. In Figure 4, a comparison is made between the spectra obtained from the clean Ru(001) and those from the Cu(2 ML)/Ru(001) surface. These spectra

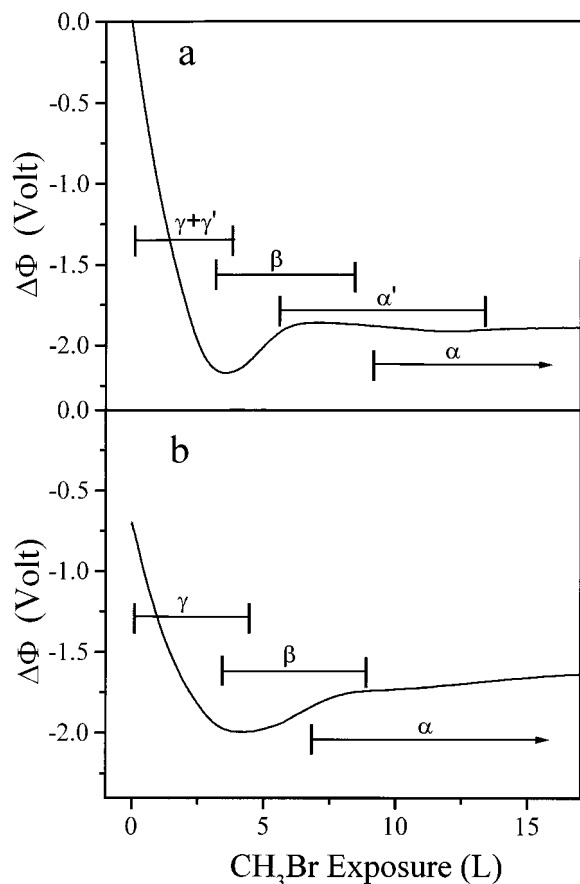


Figure 3. Work function change measurement during CH_3Br adsorption at 82 K on (a) Ru(001) and (b) Cu(2 ML)/Ru(001). The onset and completion of each desorption peak (shown in Figure 4) are indicated.

serve as indicators of the strength of interaction of the molecule with the underlying metallic surface. It is clearly seen that the ruthenium is highly reactive upon sample heating, dissociating 0.55 of the initial 1 ML of adsorbed methyl bromide. In contrast, the Cu(2 ML)/Ru(001) surface is quite inert, leading to the dissociation of only 0.06 of the initial 1 ML of CH_3Br (note the similar ordinate's scale in both insets), which is probably due to defects in the copper layer. These defects are stable even after annealing to temperatures around 1000 K.⁷⁻⁹

The γ molecular desorption peak (Figure 4), attributed to the first CH_3Br layer on the Cu(2 ML)/Ru(001) surface, shifts from 170 K at low coverages to 150 K at 1 ML because of dipole-dipole repulsion.^{29,30,35} In addition to the minor methyl bromide dissociation, 2 ML of copper reduces substantially the binding energy of the isolated CH_3Br molecule to the surface, as seen from the lower desorption temperature at low coverages. By use of a preexponential factor of $3 \times 10^{13} \text{ s}^{-1}$, the low-coverage (isolated molecule) activation energy for desorption from the copper-covered surface is 42 kJ/mol, as obtained from a full desorption line shape analysis.

Calibration of the total molecular desorption uptake obtained from the clean Ru(001)²⁹ to that from Cu(2 ML)/Ru(001) enabled the semiquantitative definition of the CH_3Br density on that surface at the completion of a monolayer. Considering the somewhat higher density of copper atoms on Cu(111), by a factor of 1.114 compared with that of ruthenium atoms on Ru(001), we came up with a density of 1 ML of methyl bromide of $\text{CH}_3\text{Br}/\text{Cu} = 0.22 \pm 0.02$ (identical to the packing on the clean Ru(001)), which translates to $(4.0 \pm 0.3) \times 10^{14}$ molecules/cm².

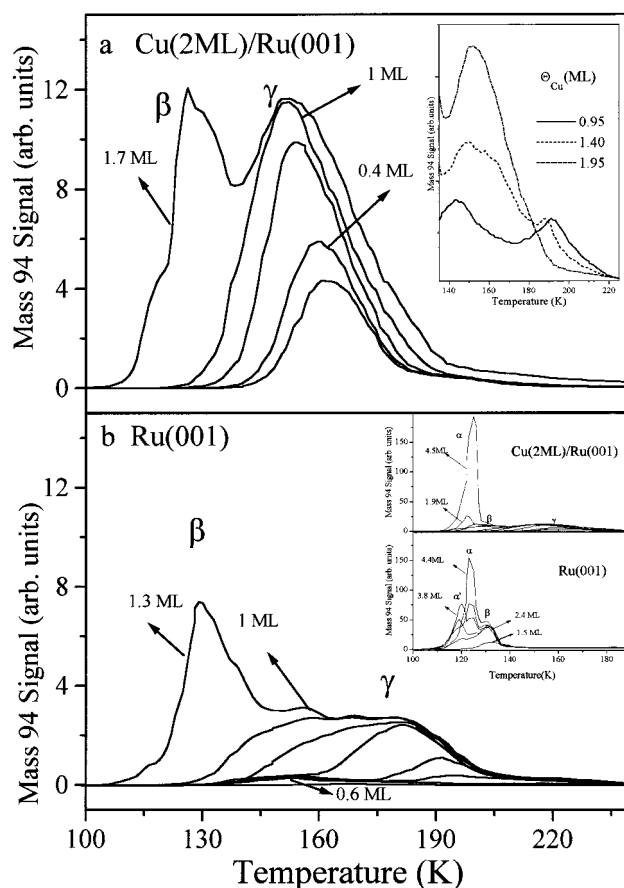


Figure 4. Δp TPD spectra of CH_3Br ($m/e = 94$) at the indicated molecular coverages from (a) Cu (2 ML)/Ru(001), 0.3–1.7 ML of CH_3Br . The inset shows Δp TPD for the indicated Cu/Ru(001) coverages and subsequent exposure to 6 L of CH_3Br . (b) Clean Ru(001), 0.1–1.3 ML of CH_3Br . The inset shows the indicated desorption spectra obtained from the multilayer methyl bromide coverage regime for Cu(2 ML)/Ru(001) and the clean Ru(001). Adsorption temperature was 82 K and the heating rate 3 K/s.

This density can then be used to estimate the low coverage (isolated molecule) dipole moment of adsorbed methyl bromide ($\mu(0)$). We obtained a dipole moment estimate $\mu(0) = 1.55 \text{ D}$ from the initial slope of work function vs coverage plot in Figure 3. This dipole moment is smaller than the gas-phase value of 1.82 D,⁴⁰ in contrast to typical cases where an adsorbed molecular state is more polarized because of the formation of surface bonding, which often results in a large dipole moment. This can be explained only on the basis of adsorption geometry arguments, which favor a significant degree of tilt of the adsorbed molecule on the Cu(2 ML)/Ru(001) surface.

Finally, in the inset of Figure 4b, the desorption spectra obtained from the multilayer methyl bromide coverage regime are shown. The β peak is centered at 130 K and is attributed to second-layer desorption. The α peak for the 2 ML Cu/Ru(001) surface is attributed to the condensed phase, and similar to the clean Ru(001), it peaks around 126 K. The sensitivity of the desorption spectra to the underlying substrate is evident. Although on the clean Ru(001) unique low-temperature desorption from a third layer (α' peak) was observed, it is absent in the desorption from the Cu(2 ML)/Ru(001) surface.

Destabilization of the third layer and then a more stable fourth and thicker layers on the clean Ru(001) has been discussed in terms of bulklike molecular crystalline structure formation.^{29,30} It turns out that on the copper-covered surface destabilization of the third layer is not observed. On the basis of the work function change spectrum during adsorption, we conclude that

on the Cu(2 ML)/Ru(001) surface, CH₃Br molecules cannot form a structure according to the molecular crystalline anti-parallel arrangement³⁴ as well as on the clean Ru(001) surface. This may be related to the fact that on this surface there are more defects, and as a result, molecules adsorb in a distribution of tilt angles with respect to the normal to the surface.

3. Cu(0–2ML)/Ru(001). *3.1. CH₃Br Desorption.* The desorption of methyl bromide from the Cu/Ru(001) surface is expected to reflect the distribution of sites shown in Figure 2. The Δp TPD spectra of CH₃Br at the monolayer coverage regime for three copper coverages between $\theta_{\text{Cu}} = 0.95$ and $\theta_{\text{Cu}} = 1.95$ are shown in the inset of Figure 4a. These spectra demonstrate the effect of copper sites on the molecular desorption. Two desorption peaks at 145 and 195 K are assigned to desorption from first-layer copper terraces (c) and copper step edges (b, d) sites, respectively. Exact assignment of each of the desorption peaks to a given site is probably impossible. These small desorption peaks change with copper coverage, and above 2 ML they coalesce into a single 155 K desorption peak, which is believed to correlate with site e in Figure 2. The activation energy from this site is 47 kJ/mol, assuming the same ($3 \times 10^{13} \text{ s}^{-1}$) preexponential factor as above. This indicates that the binding energy at the step Cu/Ru edges is 5 kJ/mol higher than the binding on the Cu(2 ML)/Ru(001) terraces.

Correlation of the work function change data obtained during desorption ($\Delta\phi$ TPD) with Δp TPD provides important and often unique information on the dependence of the dissociation mechanism of adsorbed methyl on copper coverage. The $\Delta\phi$ TPD after exposure of Cu(0–2ML)/Ru(001) surfaces to 6 L of methyl bromide at 82 K is shown in Figure 5. All changes in the work function refer to the clean Ru(001) surface and include contributions to $\Delta\phi$ due to both copper and the methyl bromide. For $\theta_{\text{Cu}} < 0.8$ ML (dashed–dotted lines) the main influence of the copper is observed between 200 and 400 K. At this temperature range the adsorbed methyl dehydrogenates almost completely to CH fragments on the clean Ru(001) surface.^{28,29} The very different $\Delta\phi$ TPD spectra caused by copper at coverages as low as 0.11 ML (not shown) indicate that the methyl dehydrogenation reaction is very sensitive to the electron density changes exerted by the adsorbed copper. The different reactivity pattern on the copper-covered, compared with the clean Ru(001) surface, is attributed to the copper step edges and their surroundings, where the dehydrogenation reaction rate of the CH₂ fragments is faster (see section 3.3 below). This statement is supported by previous reports on the special role step edges of copper on ruthenium have in, for example, slowing the diffusion of H and CO on this surface.²²

At $\theta_{\text{Cu}} \geq 0.8$ ML (solid lines), an abrupt change is observed in the $\Delta\phi$ TPD spectra. A $\Delta\phi$ decrease around 300 K disappears, and a $\Delta\phi$ rise around 400 K emerges. These results correspond to similar changes observed in the Δp TPD spectra, which mark the modification in the dehydrogenation pathway of the adsorbed methyl, as will be discussed in the next section.

Following the decomposition of parent CH₃Br and its methyl fragment using work function change measurements requires special care. This is due to the opposing effects generated by the gradual increase of the copper coverage: decreasing reactivity toward the parent molecule and its decomposition fragments but at the same time opposite $\Delta\phi$ change due to bromine atoms left on the Cu vs Ru surface.

In the inset of Figure 5, the change in $\Delta\phi$ attributed to the adsorbed fragments (carbon and bromine) left on the surface after a $\Delta\phi$ TPD run up to 550 K is shown. This is measured by subtracting the initial reading at 82 K, prior to the adsorption

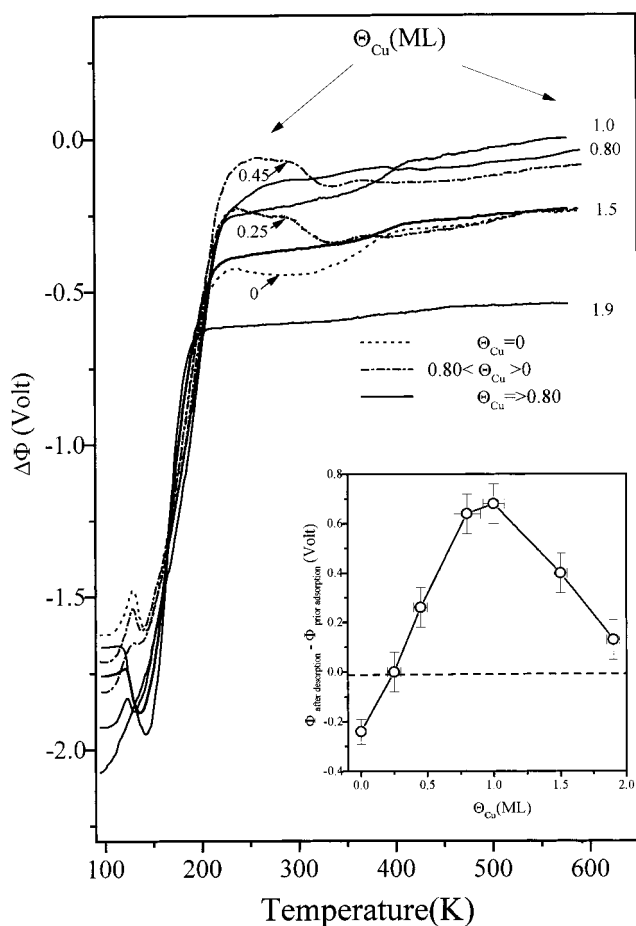


Figure 5. Work function change during temperature-programmed desorption ($\Delta\phi$ TPD) of CH₃Br from Cu(0–1.9 ML)/Ru(001) at the indicated copper coverages. The initial $\Delta\phi$ (at 82 K) comprises the $\Delta\phi$ due to adsorbed copper and subsequent exposure to 6 L of CH₃Br. In the inset, the difference between the measured $\Delta\phi$ at 82 K before exposing the surface to 6 L of CH₃Br and the one obtained at 550 K following $\Delta\phi$ TPD runs is shown. The heating rate was 2 K/s.

of 6 L of CH₃Br on the Cu/Ru(001) surface, from the $\Delta\phi$ value detected after sample heating to 550 K. Bromine forms a ($\sqrt{3} \times \sqrt{3}$)R30° structure on Cu(111).⁴¹ We assume that a similar structure is formed on both Ru(001) and Cu(2 ML)/Ru(001), defining this as 1 ML of bromine coverage (namely, 1 ML = Br/Ru = 0.33). This assumption is based on the expected similarity with the identical ordered structure formed by chlorine on Cu(111)⁴² and on Ru(001).⁴³ At 1 ML of coverage the work function change induced by bromine atoms is +0.8 and –0.32 V on Cu(111)⁴¹ and Ru(001),²⁹ respectively.

The fraction of dissociated CH₃Br gradually decreases upon increasing copper coverage. It diminishes from 0.55 of a saturated monolayer-adsorbed methyl bromide on the clean Ru(001) to 0.06 of the initial monolayer on the Cu(2 ML)/Ru(001) surface. This accounts for the amount of bromine adsorbed on the surface. The reactivity difference toward dehydrogenation of methyl groups between Ru and Cu is reflected by the decreasing amount of carbon deposited on the surface as the copper coverage increases. $\Delta\phi$ measurements following C₂H₄ decomposition have indicated that carbide atoms contribute +0.2 V for an estimated carbon coverage of C/Ru(001) of 0.11.⁴⁴

Bromine atoms left on the surface as a result of the decomposition of methyl bromide lead to a $\Delta\phi$ increase as the copper coverage grows. The work function change attributed to the adsorbed hydrocarbon fragments at 550 K reverses its

sign at $\theta_{\text{Cu}} > 0.30$ ML, and around $\theta_{\text{Cu}} = 1$ ML, the work function change is maximized at 0.68 V. The turnover and decrease of $\Delta\varphi$ at $\theta_{\text{Cu}} > 1$ ML is attributed to the gradual passivation of the surface by copper, which suppresses the molecular dissociation, resulting in a lower bromine coverage.

There is an interplay between the decreasing dissociation probability as the copper coverage increases, and the increasing work function change, due to each bromine atom that binds to copper and not to ruthenium. While on the clean Ru(001) surface the contribution of bromine atoms is negative,²⁹ as we increase the copper coverage to 1 ML, more bromine atoms adsorb on copper terraces and their step edges and contribute positively to the work function. Even at low copper coverages, where the molecules most likely dissociate on clean ruthenium sites and not at step edges of copper, the bromine atoms find their way to the nearest copper step edges, inducing positive change in $\Delta\varphi$.

In general, $\Delta\varphi$ TPD spectra reproduce rather accurately the behavior observed in the corresponding Δp TPD. One can further emphasize the similarity between these complementary methods by differentiating the $\Delta\varphi$ TPD spectra with respect to temperature, as was discussed in ref 29, and this will be demonstrated below for the desorption of methane.

3.2. CH₃ Chemistry on Cu/Ru(001). *3.2.1. CH₃/Cu(0–2ML)/Ru(001).* Two different Δp TPD signals at $m/e = 16$ (dotted lines) and $m/e = 2$ (solid lines) following the exposure of Ru(001) surfaces (covered by the indicated copper coverages $\theta_{\text{Cu}} = 0–1.95$ ML) to 6 L of CH₃Br at 82 K are shown in Figure 6. These signals reflect the catalytic production of CH₄ and H₂, respectively. The fraction of dissociated CH₃Br (sum of H₂ and total CH₄ uptake) as a function of copper coverage is summarized in Figure 7. The dissociation of CH₃Br clearly decreases with increasing copper coverage, as determined by the hydrogen uptake, which gradually vanishes, and the total methane signal, which increases as θ_{Cu} grows toward 1 ML. Around $\theta_{\text{Cu}} = 0.8$ ML, the hydrogen desorption peak develops a low-temperature tail while methane desorption at 195 K broadens toward higher temperatures. At $0.95 > \theta_{\text{Cu}} > 0.8$ ML, the hydrogen desorption disappears concomitantly with the emergence of a new desorption peak of methane centered on 370 K with a tail at 450 K. This sudden change in the adsorbed methyl dissociation pathway above 250 K at a narrow copper coverage range is seen also in the $\Delta\varphi$ TPD spectra (Figure 5) and nicely demonstrates the kind of selectivity one would expect from a bimetallic catalyst.

Hydrogen atoms were shown to “spill over” from the ruthenium terraces on top of the copper-covered areas around 130 K.⁴⁵ Our data suggest that around $\theta_{\text{Cu}} = 0.8$ ML, the adsorbed hydrogen density produced by the dissociation of the methyl species is higher than the capacity of the remaining clean Ru terraces. As a result, hydrogen “spills over” on top of the copper terraces, where it recombines with adsorbed methyl (which also reside on the copper following diffusion and “spill over” from the ruthenium sites) to produce methane. Up to $\theta_{\text{Cu}} = 0.95$ ML a regime is maintained for which adsorbed hydrogen and methyl species coexist, resulting in an overlap of their Δp TPD spectra between 230–280 K (Figure 6e). Further increase of the copper coverage above 0.95 ML results in decreased methyl radical density due to diminishing parent molecule dissociation. In addition, the methyl dissociation also gradually slows down, and thus, the hydrogen coverage is reduced. The absence of any hydrogen desorption for $\theta_{\text{Cu}} > 0.95$ ML is understood in terms of the low hydrogen coverage, which makes the recombination reaction with methyl to form methane the dominating reactivity channel.

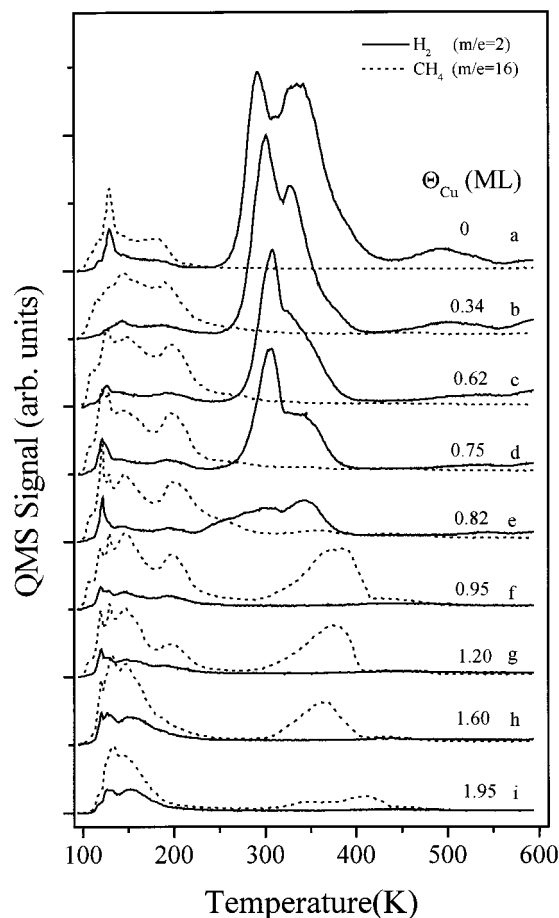


Figure 6. Δp TPD spectra at $m/e = 2$ (H₂, solid lines) and $m/e = 16$ (CH₄, dotted lines) after exposing Cu/Ru(001) surfaces at the indicated copper coverages (0–1.95 ML) to 6 L of CH₃Br. Adsorption temperature was 82 K and the heating rate 3 K/s.

Around 200 K the methane desorption rate first increases as $\theta_{\text{Cu}} \rightarrow 0.95$ ML and then it decreases again as the second copper layer starts to build up. For $\theta_{\text{Cu}} > 2$ ML methane production is practically eliminated. On the bare Ru surface, methyl dehydrogenation is faster around 200 K than the hydrogenation channel to form CH₄.²⁹ It is believed, therefore, that the desorption of methane near 200 K originates from (CH₃)_{ad} fragments at copper step edges or from those “spilled over” on top of the copper terraces. These (CH₃)_{ad} species then recombine with hydrogen atoms produced at the same temperature range from dehydrogenation of other (CH₃)_{ad} on the bare Ru sites. We note that at submonolayer copper coverages, even if methyl resides on top of the copper layer, its diffusion is fast enough to reach free Ru(001) sites and may dehydrogenate. As discussed above, the abundance of Ru sites that enable (CH₃)_{ad} dissociation is reduced at $\theta_{\text{Cu}} > 0.8$ ML (as is expressed by the hydrogen and methyl species coexistence between 230–280 K) and diminishes at $\theta_{\text{Cu}} > 0.95$ ML. Possibly, electronic structure modifications generated by the bimetallic system contribute to the reduced dehydrogenation reactivity on the Ru sites. As shown by STM measurements^{20,21} on other systems, step edges exert long-range electron density modifications on the surface (50–100 Å). If the range of these changes is similar to the average distance between the copper terraces, there will be no available Ru sites that are of pure Ru nature. Therefore, dehydrogenation of (CH₃)_{ad} is expected to be significantly perturbed and eventually be totally blocked. This can be understood in terms of an “ensemble” effect in the surface reactivity of the methyl fragments.

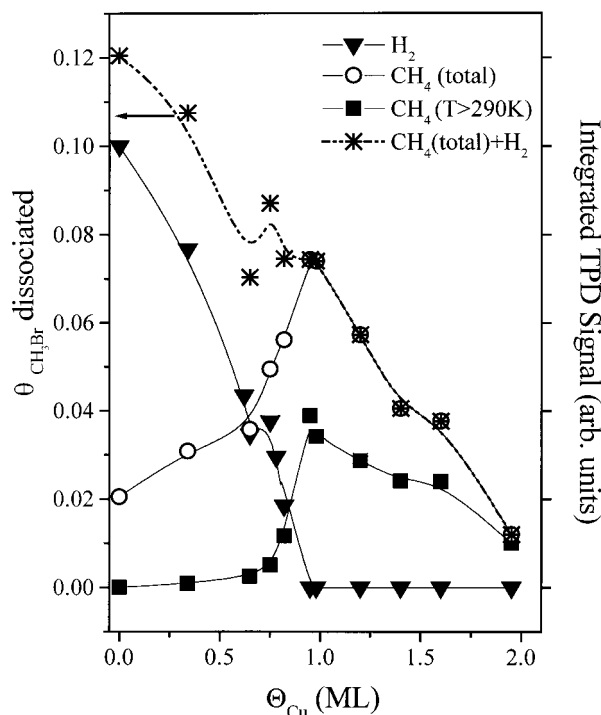


Figure 7. Extent of CH₃Br fragmentation ($\theta = \text{CH}_3\text{Br}/\text{Ru}(001) = 0.22 \pm 0.02$ at 1 ML) as a function of copper coverage, reflected by the integrated area under the hydrogen ($m/e = 2$) and methane ($m/e = 16$) Δp TPD signals shown in Figure 6.

$\Delta\phi$ TPD spectra at $\theta_{\text{Cu}} > 0.8$ ML (Figure 5) reveal a monotonic increase of the work function before and during the desorption of methane around 370 K. This slow increase can be interpreted as the contribution of partial (diminishing) decomposition of the methyl and its products that results in the accumulation of hydrogen and possibly carbon atoms on the surface. The production of methane from the recombination of methyl radicals and hydrogen atoms was previously reported to take place on Cu(110)⁴⁶ around 380 K, in good agreement with the 370 K peak temperature observed in Figure 6. The recombination reaction to form methane is a second-order reaction that should shift to lower temperatures with increasing methyl radical and atomic hydrogen density. However, as seen in Figure 6, with decreasing copper coverages a clear shift to *higher* temperatures is observed with a common leading edge. This reaction scheme, therefore, is not consistent with a simple elementary second-order kinetics. It can, however, be rationalized as a pseudo-first-order reaction with excess methyl radical concentration. The hydrogen is apparently produced by dehydrogenation of the fraction of the methyl adsorbates as the *rate-limiting step* followed by a fast hydrogen–methyl recombination reaction to form methane. Since the rate constants for hydrogen recombination and methyl radical hydrogenation are comparable,⁴⁶ the absence of hydrogen desorption indicates that its concentration is negligible throughout the course of the reaction and supports the above interpretation. When copper coverage approaches 2 ML, less hydrogen is produced because of passivation of the surface toward methyl dissociation, as discussed above.

X-ray photoelectron spectroscopy (XPS)¹⁶ and photoemission of adsorbed xenon (PAX)¹⁷ studies of the Cu/Ru(001) system have revealed strong electronic perturbations at the first copper monolayer coverage range. These perturbations are held responsible for the higher reactivity of the Cu(1 ML)/Ru(001) relative to the Cu(2 ML)/Ru(001). The ability of the transition metal to chemically activate noble metal atoms is well-known

in heterogeneous catalysis^{15a} and has recently been discussed theoretically on the basis of d electron occupation using density functional theory.^{15b} For example, the rate of cyclohexene dehydrogenation is 6-fold-enhanced on the Au(1 ML)/Pt(100) surface compared to the Pt(100) surface.¹⁴ Coverages of 2 ML of Au on Pt(100) were found, however, to deactivate the surface. In a similar way, our results indicate that 1 ML of Cu is not sufficient to deactivate the Ru(001) surface for both CH₃Br and CH₃ dissociation. Only upon second-layer Cu deposition is the Ru surface practically passivated (besides dissociation at defect sites). Copper deposition beyond 2 ML (checked specifically for coverages up to 5 ML) causes further increase of the surface work function by 0.08 V, toward that of Cu(111),^{25a} with no substantial change in the surface reactivity. We conclude that the surface work function, which responds to bond polarization at the first monolayer regime, is not sensitive enough as a probe of surface reactivity beyond 1 ML of deposition.

It is worthwhile to compare the methyl chemistry on Cu(1 ML)/Ru(001) with that on Cu(110)⁴⁶ and Cu(111),^{31,47} where it was prepared from CH₃I dissociation. A detailed study of these surfaces have found methyl radicals to be stable up to 400 K, where they disproportionate to form mainly methane and ethylene with the same first-order kinetics and the same desorption rate, with a peak desorption temperature around 460 K. The rate-determining step is the dissociation of CH₃ to CH₂ and H. At higher methyl coverages ethane (C₂H₆) is also produced around 450 K by CH₃ coupling with pronounced second-order kinetics features. This channel has a threshold methyl coverage $\theta_{\text{CH}_3} > 0.015$.⁴⁶

Methyl radical dissociation was shown to strongly depend on the hydrogen surface coverage. When a Cu(110) surface covered by adsorbed methyl is exposed to deuterium atoms (produced by a hot filament), most of the methyl radicals have desorbed around 380 K as CH₃D,⁴⁶ prior to the methyl decomposition, which takes place at $T > 400$ K. In the present study, at θ_{Cu} in the range 1–2 ML, the hydrogen atoms are supplied by methyl dehydrogenation either on the Ru sites, which are exposed through defects in the copper layer, or on the Cu(1 ML)/Ru(001) terraces, as a result of methyl dissociation. Both lead to methyl hydrogenation to form methane around 370 K, similar to the chemistry on Cu(110).⁴⁶

3.2.2. CH₃/Cu(1 ML)/Ru(001) vs CH₃/Cu(2 ML)/Ru(001). Unlike CH₃I, methyl bromide does not dissociate at all on Cu(111),^{32,33} and only a small fraction dissociates on Cu(2 ML)/Ru(001). Consequently, the chemistry of methyl on these surfaces (in the absence of coadsorbed hydrogen atoms) cannot be studied by simple thermal excitation. To produce a high density of methyl radicals on the surface, we had to apply other means to dissociate the parent molecule. This was achieved by exposing the CH₃Br/Cu(2 ML)/Ru(001) system to UV light from a xenon lamp (450 W) with a wavelength range of 230–420 nm. Photodissociation of CH₃Br to CH₃ and Br is rather facile.^{33,39} Adsorbed methyl groups on Cu(2 ML)/Ru(001) were thus formed at an equivalent coverage of 0.18 of the initial 1 ML of methyl bromide and then react to form methane and desorb around 460 K. This is similar to the outcome of the thermal dissociation of CH₃I on Cu(111).³¹ Halides at low coverages do not affect the rate of methane formation and its desorption temperature from copper surfaces.^{46,47} The influence of the underlying Ru on the reaction between methyl fragments on copper can be studied most conveniently by a comparison between the chemistry on Cu(1 ML)/Ru(001) to that on Cu(2 ML)/Ru(001).

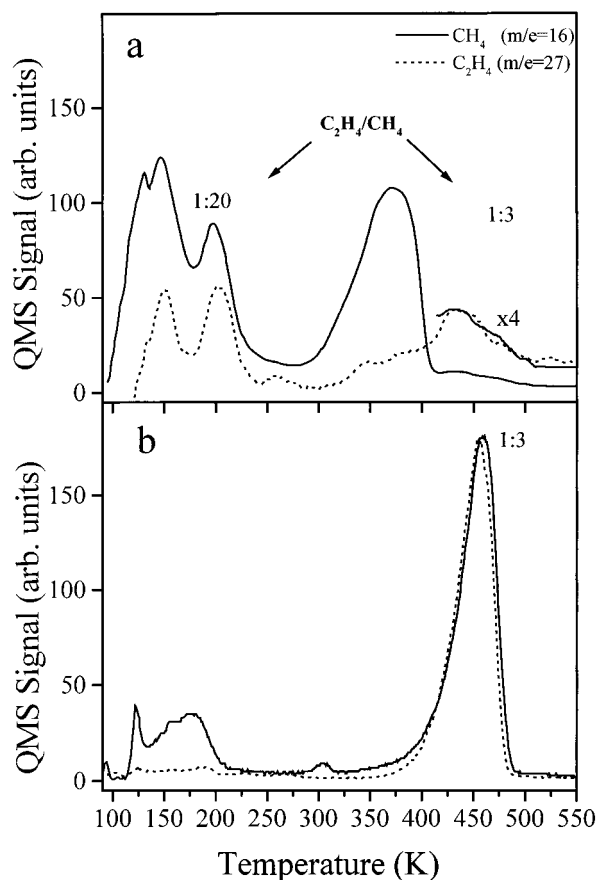


Figure 8. Δp TPD spectra of CH_4 (solid line) and C_2H_4 (dotted line) (a) after exposing $\text{Cu}(0.95 \text{ ML})/\text{Ru}(001)$ surface to 6 L of CH_3Br . The tail above 400 K is 4-fold-magnified. (b) After covering a $\text{Cu}(2 \text{ ML})/\text{Ru}(001)$ surface by 1 ML of CH_3Br (4 L exposure) followed by 24 min of broad-band UV (230–420 nm) irradiation from a 450 W Xe lamp.

In Figure 8 we compare the temperature-programmed methane production (solid lines) from $\text{Cu}(0.95 \text{ ML})/\text{Ru}(001)$ (Figure 8a) to that from $\text{Cu}(2 \text{ ML})/\text{Ru}(001)$ (Figure 8b). Methyl fragments are generated by thermal dissociation of the parent CH_3Br molecule on $\text{Cu}(0.95 \text{ ML})/\text{Ru}(001)$ and via photochemical decomposition on $\text{Cu}(2 \text{ ML})/\text{Ru}(001)$. A small fraction of the methyl fragments react through a competing channel to form ethylene, as shown in the dotted lines. No C_2H_6 molecules are produced on both copper-covered surfaces. This can be explained by the need for higher methyl coverage in order to initiate a methyl coupling reaction to form ethane, as was found on $\text{Cu}(111)^{31,47}$ and $\text{Cu}(110)^{46}$.

Several important differences are noted in the methyl reactivity on the two copper-covered surfaces. On $\text{Cu}(0.95 \text{ ML})/\text{Ru}(001)$ (Figure 8a) the production and desorption peak of CH_4 (370 K) appears at lower temperature and it does not overlap the minor ($\sim 0.003 \text{ ML}$) ethylene desorption peak. The desorption profiles of methane and ethylene at 460 K from $\text{Cu}(2 \text{ ML})/\text{Ru}(001)$, however, exactly overlap, as seen in Figure 8b. On both copper coverages the ethylene/methane ratio above 400 K is 1:3. This observation suggests that at these temperatures methane and ethylene are produced via the same mechanism: methyl disproportionation on top of the copper terraces, as was shown before to be the mechanism on $\text{Cu}(110)$ and $\text{Cu}(111)^{31,46,47}$. The intensity ratio of 1:20 for $\text{C}_2\text{H}_4/\text{CH}_4$ observed at the methane desorption peak near 200 K (Figure 8a) indicates that the mechanism that leads to ethylene production at this temperature range is different; ethylene was shown to be formed on copper

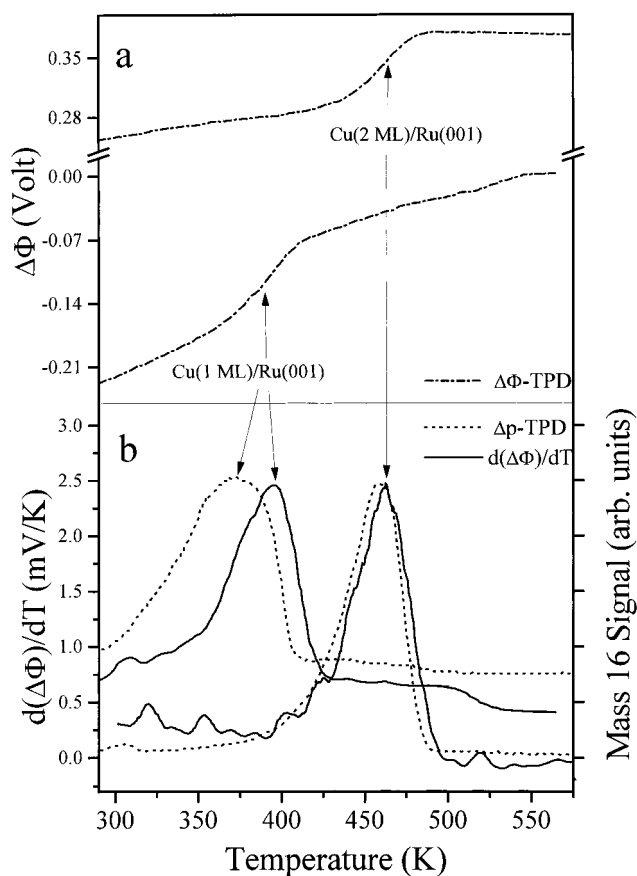


Figure 9. (a) $\Delta\phi$ TPD (dashed–dotted lines) and (b) Δp TPD (dotted lines) and $d(\Delta\phi)/dT$ (solid lines) spectra after exposing $\text{Cu}(1 \text{ ML})/\text{Ru}(001)$ surface to 6 L of CH_3Br . The same is also measured on a $\text{Cu}(2 \text{ ML})/\text{Ru}(001)$ surface covered by 1 ML of CH_3Br (4 L exposure) and followed by 24 min of broad-band UV (230–420 nm) irradiation from a 450 W Xe lamp.

surfaces also by methylene coupling ($2\text{CH}_2 \rightarrow \text{C}_2\text{H}_4$) around 200–230 K.^{46,48} Methylene groups may be formed at copper step edges where higher reactivity toward CH_3 dehydrogenation is expected with subsequent “spill over” on top of the copper terraces. This channel is gradually eliminated upon second copper layer deposition (not shown). Finally, we note the small methane peak produced on $\text{Cu}(2 \text{ ML})/\text{Ru}(001)$, as seen in Figure 8b around 300 K without any ethylene formation. This peak is attributed to a recombination of hydrogen (produced at surface defects) with methyl radicals.⁴⁶ Production of methane at the same temperature was previously observed after photochemical decomposition of CH_3Br on $\text{Cu}(10 \text{ ML})/\text{Ru}(001)$ as well.³⁹

The effect of the underlying ruthenium atoms on the reaction of methyl species on top of the copper terraces can also be studied by measuring the work function change during methane formation and desorption between 300 and 500 K, employing a $\Delta\phi$ TPD mode. In Figure 9a, $\Delta\phi$ measurements during methane production on $\text{Cu}(2 \text{ ML})/\text{Ru}(001)$ are shown for photochemically produced CH_3 (upper curve) and for thermally produced $\text{CH}_3 + \text{H}/\text{Cu}(1 \text{ ML})/\text{Ru}(001)$ (lower curve). Before and after the methane desorption, only a small change in the work function is observed on the $\text{Cu}(2 \text{ ML})/\text{Ru}(001)$ surface. In contrast, in the $\text{Cu}(1 \text{ ML})/\text{Ru}(001)$ case, a continuous increase in the work function of about 0.7 mV/K, prior to desorption, is observed. This rate of increase scales with the amount of methane that desorbs around 370 K (not shown). Therefore, we attribute this increase to methyl fragmentation on the copper monolayer followed by accumulation of hydrogen atoms on the surface. This hydrogen, however, is not in high enough density

to recombine and desorb as H₂ at temperatures below the desorption of methane.

A comparison of the Δp TPD and the $d(\Delta\varphi)/dT$ spectra is shown in Figure 9b. For the Cu(2 ML)/Ru(001) case there is a very good overlap between the two spectra. This is not surprising, considering that we actually follow the rate-determining step, which is methyl dissociation ($\text{CH}_3 \rightarrow \text{CH}_2 + \text{H}$).^{46,47} The reactions of methylene insertion and methyl hydrogenation were found to be considerably faster than methyl dissociation on Cu(110).⁴⁶ Therefore, further decomposition of the methylene fragments must take place simultaneously with the methyl fragmentation without affecting the measured work function change.

The work function increases by 0.12 V upon the removal of methyl species from Cu(2 ML)/Ru(001). On the basis of the integrated area under the corresponding methane Δp TPD peak, the photochemically generated methyl coverage reached $\text{CH}_3/\text{Cu} = 0.04$ ML (0.18 of an initial 1 ML of methyl bromide). Simple calculation based on the Helmholtz equation, $\Delta\varphi = 4\pi N\mu_0$, where N is the surface methyl density and μ_0 is the isolated methyl dipole moment, provides an estimate of the isolated adsorbed methyl dipole moment of $\mu_0 = 0.48$ D (1 D = 3.34×10^{-30} C m). The justification to use this simplified model stems from the low coverage and insignificant dipole-dipole interaction between the methyl adsorbates.

Unlike the Cu(2 ML)/Ru(001) surface, at the lower coverage of Cu(1 ML)/Ru(001), the $d(\Delta\varphi)/dT$ spectrum does not overlap the Δp TPD. The $d(\Delta\varphi)/dT$ peak shifts to higher temperatures by 25 K with respect to the Δp TPD spectrum. A similar peak temperature shift (26 K) is also observed for Cu(1.5 ML)/Ru(001). The origin of this temperature shift is not well understood. Taking into account the low concentration of methyl species, we exclude dipole-dipole interactions as the origin of this lack of overlap between the two spectra. The enhanced dissociation of the methyl fragments prior to methane desorption, which results in the sudden rise in surface coverage of methylene and hydrogen species, is not a feasible explanation as well. This is due to the absence of detectable ethylene desorption at these temperatures (see Figure 8a), expected to reflect the presence of methylene fragments on the surface. Higher density of carbon deposits may explain the observed difference. Further investigation of this issue is required.

3.3. CH₂/Cu(0–1ML)/Ru(001). The dehydrogenation pathway of CH₃Br/Ru(001)²⁹ was shown to correlate well with the suggested scheme for CH₃I/Ru(001).²⁸ By combination of the work function change and Δp TPD data, additional insight could be gained. Similar information has been obtained for the copper-covered ruthenium. A comparison between the hydrogen desorption signal obtained at various copper coverages (Figure 10a) and their corresponding $\Delta\varphi$ TPD spectra (Figure 10b) is presented. The CH₂ fragments that are left on the surface in the presence of copper at temperatures higher than 210 K display a different $\Delta\varphi$ TPD profile during their dissociation than on the clean Ru(001) surface. Between the clean and 0.45 ML copper-covered Ru(001) surfaces a peak emerges in the $\Delta\varphi$ TPD between 280 and 320 K. The dissociation pathway changes already at very low copper coverages $\theta_{\text{Cu}} = 0.11$, and at least part of it occurs at sites that are localized around the copper step edge boundary (sites b in Figure 2). At the same time, the high-temperature Δp TPD peak of hydrogen near 310 K decreases significantly. This hydrogen peak is attributed to a combination of ethylidene (CCH₃) dissociation and recombinative desorption of hydrogen.^{28,29} The faster decay of this 310 K Δp TPD peak relative to the 280 K peak may be explained by

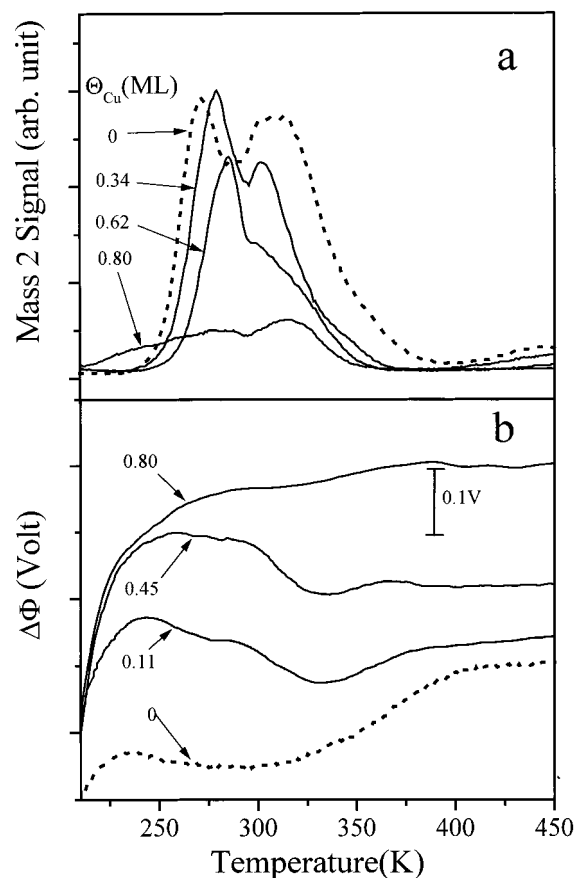


Figure 10. Comparison between (a) Δp TPD of hydrogen and (b) $\Delta\varphi$ TPD after exposing Ru(001) surface covered by the indicated copper coverage (0–0.80 ML) to 6 L of CH₃Br. For reasons of clarity, the $\Delta\varphi$ TPD spectra are shifted upward without a true representation of the $\Delta\varphi$ values.

the lower rate of ethylidene formation from recombination between two CH₂ groups^{28,29} as the copper coverage increases. This is consistent with the restricted diffusion of the CH₂ fragments due to their capture at the step edges of the growing copper layers.²² Finally, the $\Delta\varphi$ TPD profile around 300 K suddenly changes at about $\theta_{\text{Cu}} = 0.8$ ML, which correlates well with the onset of methane formation detected at 370 K in the Δp TPD spectra shown in Figure 6.

IV. Conclusions

CH₃Br/Cu/Ru(001) is an interesting model system to investigate the chemistry of methyl halides on bimetallic catalysts for the following reasons. (a) Cu is immiscible in Ru, and its overlayer structure is well established in the coverage range $\theta_{\text{Cu}} = 0$ –4 ML. (b) The different reactivity of CH₃Br on single-crystal copper (no dissociation) vs Ru(001) surface (55% dissociation) enables the gradual change in reactivity with growing copper coverage.

The chemistry of CH₃Br on Cu/Ru(001) has been studied utilizing work function change ($\Delta\varphi$) and TPD measurements. A decrease in work function at the completion of 1 ML of CH₃Br of 2.15 ± 0.02 eV and 1.33 ± 0.05 eV have been measured, respectively, for Ru(001) and Cu(2 ML)/Ru(001) held at 82 K. Methyl bromide does not dissociate upon adsorption on the clean or the copper-covered ruthenium surfaces, and it is bound with the bromine down at coverages below the completion of the first monolayer.

Copper inhibits the dissociation of CH₃Br on Ru(001) and modifies the dehydrogenation pathway of the methyl fragment.

As copper atoms gradually block ruthenium sites, a decrease in the extent of methyl dehydrogenation is observed. Thus, the accumulation of methyl fragments gradually enhances the formation and desorption of methane on account of hydrogen.

In the copper coverage range 0.8–0.95 ML, adsorbed hydrogen and methyl coexist on the surface in the temperature range 230–280 K, as revealed by the Δp TPD of both hydrogen and methane. It indicates that the methyl species “survive” on the Cu/Ru(001) surface at a temperature range where it would have been completely dehydrogenated on the bare ruthenium surface. Near the completion of one copper monolayer, hydrogen desorption completely terminates. It marks a significant decrease in CH₃ dehydrogenation rate due to insufficient area of bare ruthenium active sites.

In contrast to the information obtained from work function change measurements, reactivity of the first pseudomorphic copper layer is significant toward methyl bromide and methyl dissociation. At θ_{Cu} in the range 1–2 ML with 1 ML of CH₃Br on top, $\Delta\phi$ TPD measurements indicate a continuous increase at temperatures below any hydrogen or methane desorption around 370 K. This work function increase is attributed to a continuous decomposition of the methyl and its fragments, becoming the hydrogen source for the methyl–hydrogen recombination reaction to form methane. Upon completion of the second copper layer the Ru(001) surface is passivated and only 0.06 out of a monolayer of CH₃Br dissociates, probably because of defects.

Acknowledgment. We thank Ch. Ammer and H. Neddermeyer for providing us the STM image shown in Figure 1. This research has been partially supported by a grant from G.I.F., the German–Israeli Foundation for Scientific Research and Development, The Israel Science Foundation, and the James Franck Program. The Farkas Center for Light Induced Processes is supported by the Bundesministerium für Forschung und Technologie and the Minerva Gesellschaft für die Forschung mbH.

References and Notes

- Sinfelt, J. H. *Bimetallic catalysts: discoveries, concepts and applications*; Wiley: New York, 1983.
- Sinfelt, J. H. *Acc. Chem. Res.* **1977**, *10* and references therein.
- Bond, G. C.; Turnham, B. D. *J. Catal.* **1976**, *45*, 128.
- Wu, X.; Gerstein, B. C.; King, T. S. *J. Catal.* **1990**, *121*, 271.
- Vannice, M. A. *J. Catal.* **1975**, *37*, 449.
- Vannice, M. A. *J. Catal.* **1975**, *37*, 462.
- Pötschke, G.; Schröder, J.; Günther, C.; Hwang, R. Q.; Behm, R. *J. Surf. Sci.* **1991**, *251/252*, 592.
- (a) Günther, C.; Vrijmoeth, J.; Hwang, R. Q.; Behm, R. *J. Phys. Rev. Lett.* **1995**, *74*, 754. (b) Pötschke, G.; Behm, R. *J. Phys. Rev. Lett.* **1991**, *44*, 1442.
- (9) Ammer, Ch. Private communication. (b) Ammer, Ch.; Meinel, K.; Wolter, H.; Beckmann, A.; Neddermeyer, H. *Surf. Sci.* **1997**, *375*, 302.
- (10) Yates, J. T., Jr.; Peden, C. H. F.; Goodman, D. W. *J. Catal.* **1985**, *94*, 576.
- Park, C.; Bauer, E.; Popa, H. *Surf. Sci.* **1987**, *187*, 86.
- Vickerman, J. C.; Christmann, K.; Ertl, G. *J. Catal.* **1981**, *71*, 175.
- Campbell, C. T. *Annu. Rev. Phys. Chem.* **1990**, *41*, 775.
- Sachtler, J. W. M.; Biberian, J. P.; Somorjai, G. A. *Surf. Sci.* **1981**, *110*, 43.
- (15) Goodman, D. W. *J. Phys. Chem.* **1996**, *100*, 13090 and references therein. (b) Besenbacher, F.; Chorkendorff, I.; Clausen, B. S.; Hammer, B.; Molenbroek, A. M.; Nørskov, J. K.; Stensgaard, I. *Science* **1998**, *279*, 1913.
- (16) Rodriguez, J. A.; Campbell, R. A.; Corneille, J.S.; Goodman, D. W. *Chem. Phys. Lett.* **1991**, *180*, 139.
- (17) Kim, K. S.; Sinfelt, J. H.; Eder, S.; Market, K.; Wandelt, K. *J. Phys. Chem.* **1987**, *91*, 2337.
- (18) Wandelt, K. In *Physics and Chemistry of Alkali Metal Adsorption*; Bonzel H. P., Bradshaw A. M., Ertl G., Eds.; Elsevier: Amsterdam, 1989; p 25.
- (19) Kalki, K.; Pennemann, B.; Schröder, U.; Heichler, W.; Wandelt, K. *Appl. Surf. Sci.* **1991**, *48/49*, 59.
- (20) Avouris, P.; Lyo, I-W.; Walkup, R. E. *J. Vac. Sci. Technol. B* **1994**, *12*, 1447.
- (21) Crommie, M. F.; Lutz, C. P.; Eigler, D. M. *Nature* **1993**, *363*, 524.
- (22) Brown, D. E.; Sholl, D. S.; Skodje, R. T.; George, S. M. *Chem. Phys.* **1996**, *205*, 23.
- (23) Christmann, K.; Ertl, G.; Shimizu, H. *J. Catal.* **1980**, *61*, 397.
- (24) Houston, J. E.; Peden, C. H. F.; Blair, D.S.; Goodman, D. W. *Surf. Sci.* **1986**, *167*, 427.
- (25) Wolter, H.; Schmidt, M.; Wandelt, K. *Surf. Sci.* **1993**, *298*, 173.
- (b) Campbell, C. T. *Annu. Rev. Phys. Chem.* **1990**, *41*, 775.
- (26) Sakakini, B.; Swift, A. J.; Vickerman, J. C.; Harendt, C.; Christmann, K. *J. Chem. Soc., Faraday Trans. 1* **1987**, *83*, 1975.
- (27) Dubois, L. H.; Bent, B. E.; Nuzzo, R. G. In *Surface Reactions*; Madix, R. J., Ed.; Springer Series in Surface Science 34; Springer-Verlag: Berlin, 1994; p 135.
- (28) Zhou, Y.; Henderson, M. A.; Feng, W. M.; White, J. M. *Surf. Sci.* **1989**, *224*, 386.
- (29) Livneh, T.; Asscher, M. *J. Phys. Chem.* **1997**, *B101*, 7505.
- (30) Livneh, T.; Asscher, M. *Langmuir* **1998**, *14* (6), 1348.
- (31) Lin, J.-L.; Bent, B. E. *J. Vac. Sci. Technol.* **1992**, *10* (4), 2202.
- (32) Lin, J.-L.; Bent, B. E. *J. Phys. Chem.* **1992**, *96*, 8529.
- (33) Lamont, C. L. A.; Conrad, H.; Bradshaw, A. M. *Surf. Sci.* **1993**, *280*, 79.
- (34) Kawaguchi, T.; Hijikigawa, M.; Hayafuji, Y.; Ikeda, M.; Fukushima, R.; Tomiie, Y. *Bull. Chem. Soc. Jpn.* **1973**, *46*, 53.
- (35) Maschhoff, B. L.; Cowin, J. P. *J. Chem. Phys.* **1994**, *101* (9), 8138.
- (36) Redhead P. A. *Vacuum* **1962**, *12*, 203.
- (37) French, C.; Harrison, I. *Surf. Sci.* **1995**, *342*, 85.
- (38) French, C.; Harrison, I. *Surf. Sci.* **1997**, *387*, 11.
- (39) Roop, B.; Zhou, Y.; Liu, Z.-M.; Henderson, M. A.; Lloyd, K. G.; Campion, A.; White, J. M. *J. Vac. Sci. Technol.* **1989**, *A7*, 2121.
- (40) *Handbook of Chemistry and Physics*, 76th ed.; Lide, D. R., Ed.; CRC: Boca Raton, FL, 1995.
- (41) Bange, K.; Dohl, R.; Grindler, D. E.; Sass, J. K. *Vacuum* **1983**, *33* (10–12), 757.
- (42) Goddard, P. J.; Lambert, R. M. *Surf. Sci.* **1977**, *67*, 180.
- (43) Preyss, W.; Ebinger, H. D.; Fick, D.; Polenz, C.; Polivka, B.; Saier, V.; Veith, R.; Weindel, Ch.; Jansch, H. *J. Surf. Sci.* **1997**, *373*, 33.
- (44) Livneh, T.; Asscher, M. Submitted for publication.
- (45) Goodman, D. W.; Yates, J. T., Jr.; Peden, C. H. F. *Surf. Sci.* **1985**, *164*, 417.
- (46) Chiang, C.-M.; Wentzlaff, T. H.; Bent, B. E. *J. Phys. Chem.* **1992**, *96*, 1836.
- (47) Chiang, C.-M.; Bent, B. E. *Surf. Sci.* **1992**, *279*, 79.
- (48) Kovács, I.; Solymosy, F. *J. Phys. Chem. B* **1997**, *101*, 5397.